Available online at www.sciencedirect.com
ScienceDirect
Catalysis Today 120 (2007) 281–286
CATALYSIS TODAY
www.elsevier.com/locate/cattod

Hydrogen-storage properties of a Mg-based mixture prepared by reactive mechanical grinding with ultrafine Fe_2O_3 particles and Ni

MyoungYoup Song [a,*], SungNam Kwon [a], Seong-Hyeon Hong [b], ChanGi Park [a], SungHwan Baek [a], HyoSuk Kim [a], Daniel R. Mumm [c], Jong-Soo Bae [b]

[a] *Division of Advanced Materials Engineering, Research Center of Advanced Materials Development, Engineering Research Institute, Chonbuk National University, 664-14 1ga Deogjindong Deogjingu, Jeonju, Chonbuk 561-756, Republic of Korea*
[b] *Powder Materials Research Center, Korea Institute of Machinery & Materials, 66 Sangnamdong, Changwon, Kyungnam 641-010, Republic of Korea*
[c] *Department of Chemical Engineering and Materials Science, University of California, Irvine, CA 92697-2575, USA*

Available online 7 November 2006

Abstract

The sample Mg-10 wt.% (Fe_2O_3, Ni) was prepared by grinding Mg mechanically under H_2 (reactive mechanical grinding) with ultrafine Fe_2O_3 particles and Ni particles. The sample Mg-10 wt.% (Fe_2O_3, Ni) as milled absorbed 4.24 wt.% hydrogen at 593 K under 12 bar H_2 for 60 min. Its activation was accomplished only by one hydriding–dehydriding cycle. The activated sample absorbed 4.05 wt.% hydrogen at 593K, 12 bar H_2 for 60 min and desorbed 3.05 wt.% hydrogen at 593 K, 1.0 bar H_2 for 60 min. After hydriding–dehydriding cycling, Fe_2O_3 was reduced, Mg_2Ni was formed by the reaction of Mg with Ni, and a small fraction of Mg was oxidized.

Keywords: H_2-sorption properties of Mg; Addition of ultrafine Fe_2O_3 and Ni; Reactive mechanical grinding; Reduction of Fe_2O_3; Mg_2Ni formation; Oxidation of Mg; Catalytic role of Mg_2NiH_4 for the decomposition of MgH_2

1. Introduction

Magnesium has many advantages for a hydrogen-storage material: large hydrogen-storage capacity (7.6 wt.%), low cost, and abundance in the earth's crust. However, its hydriding and dehydriding kinetics are very slow. A lot of works to ameliorate the reaction kinetics of magnesium with hydrogen have been done by alloying certain metals with magnesium, mixing metal additives with magnesium, or plating nickel on the surface of magnesium.

Song [1] reviewed the kinetic studies of the hydriding and the dehydriding reactions of Mg. Many works do not agree with one another on the rate-controlling step(s) for hydriding or dehydriding reactions of magnesium. However, there is no contradiction in the points that the hydriding and dehydriding reactions of Mg are nucleation-controlled under certain conditions and progress by a mechanism of nucleation and growth, and that the hydriding rates of Mg are controlled by the diffusion of hydrogen through a growing Mg-hydride layer.

The hydriding and dehydriding kinetics of Mg can be improved, therefore, by a treatment such as mechanical alloying [2–4] which can facilitate nucleation by creating many defects on the surface and/or in the interior of Mg, or by the additive acting as active sites for the nucleation, and shorten diffusion distances by reducing the effective particle sizes of Mg.

Bobet et al. [5] reported that mechanical alloying in H_2 (reactive mechanical grinding) for a short time (2 h) was an effective way to improve significantly the hydrogen-storage properties of both magnesium and Mg + 10 wt.% Co, Ni or Fe mixtures. Klassen and co-workers [6], Huot et al. [7] and Imamura et al. [8] improved hydrogen-sorption kinetics of magnesium by adding metal, oxide or carbon through mechanical grinding.

The oxides are brittle, and thus they may be pulverized during mechanical grinding. The added oxides and/or their pulverization during mechanical grinding may help the particles of magnesium become finer.

Our previous work studied the optimum conditions for the preparation of the sample Mg-10 wt.% Fe_2O_3 using purchased

* Corresponding author. Tel.: +82 63 270 2379; fax: +82 63 270 2386.
E-mail address: songmy@chonbuk.ac.kr (M. Song).

0920-5861/$ – see front matter © 2006 Elsevier B.V. All rights reserved.
doi:10.1016/j.cattod.2006.09.017

Fe_2O_3 by reactive mechanical grinding. The optimum conditions were the disc revolution speed of 250 rpm, the milling time of 2 h and the sample to ball weight ratio of 1/45 [9].

In our previous work [10], we also studied hydrogen-sorption properties of Mg-10 wt.% oxide prepared by reactive mechanical grinding. Among these samples, Mg-10 wt.% Fe_2O_3 prepared by spray conversion had the highest hydriding rate. The addition of Ni or Co to Mg increased greatly the hydriding and dehydriding rates of Mg [11–15].

In this work, we designed a sample with a composition of 90 wt.% Mg, 5 wt.% Fe_2O_3 prepared by spray conversion and 5 wt.% Ni purchased. We designated this sample Mg-10 wt.% (Fe_2O_3, Ni). This composition was chosen because the addition of Fe_2O_3 was considered to be able to increase the hydriding rate of Mg, and the addition of Ni to be able to increase the hydriding and dehydriding rates of Mg. The samples were prepared by reactive mechanical grinding, and their hydrogen-storage properties were then investigated.

2. Experimental details

Pure Mg powder (particle size 50 μm) was mixed with ultrafine particles Fe_2O_3 (36 nm) prepared by spray conversion, and Ni (∼5 μm average, purity 99.9%, CERAC) (total weight, 8 g) in a stainless steel container (with 105 hardened steel balls, total weight = 360 g) sealed hermetically. All sample handling was performed in a glove box under Ar in order to prevent oxidation. The mill container was then filled with high purity hydrogen gas (≈10 bar). The disc revolution speed was 250 rpm and the milling time was 2 h. These reactive mechanical grinding conditions (the sample to ball weight ratio, the disc revolution speed and the milling time) were the optimum ones for the preparation of Mg-10 wt.% Fe_2O_3 using the purchased Fe_2O_3.

The hydriding apparatus was described previously [16]. The absorbed or desorbed hydrogen quantity was measured as a function of time by a volumetric method. X-ray diffraction (XRD) analysis was carried out for the as-milled powders and for the samples after hydriding–dehydriding cycling. The microstructures were observed by scanning electron microscope (SEM).

3. Results and discussion

Fig. 1 shows the X-ray (Cu Kα) powder diffraction pattern of Mg-10 wt.% (Fe_2O_3, Ni) as milled with the sample to ball weight ratio 1/45 at the revolution speed 250 rpm for 2 h. A small amount of MgH_2 was formed in the sample. The sample also contains Fe_2O_3 and Ni, the most part of the sample being Mg.

Fig. 2 gives the microstructure observed by SEM of Mg-10 wt.% (Fe_2O_3, Ni) as milled, at different magnifications. The sample contains small particles and large particles with very small particles on their surfaces.

Fig. 3 shows the variation of weight percentage of hydrogen H_a absorbed by Mg-10 wt.% (Fe_2O_3, Ni) as a function of time t at 593 K under 12 bar H_2 according to the number of cycles n.

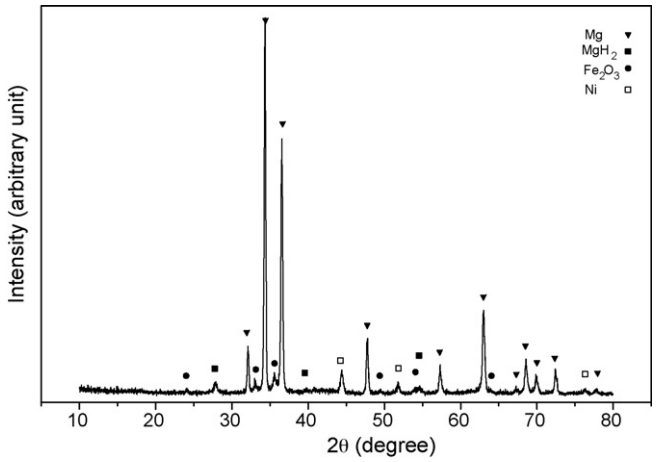

Fig. 1. X-ray (Cu Kα) powder diffraction pattern of Mg-10 wt.% (Fe_2O_3, Ni) as milled.

The percentage of absorbed hydrogen H_a is expressed with respect to the sample weight. The sample Mg-10 wt.% (Fe_2O_3, Ni) as milled absorbed 4.24 wt.% hydrogen at 593 K under 12 bar H_2 for 60 min. As the number of cycles increases the hydriding rate becomes higher. The H_a versus t curves for $n = 2$ and 3 are very similar, indicating that the activation is completed at $n = 1$.

Fig. 4 shows the H_a versus t curves for the activated Mg-10 wt.% (Fe_2O_3, Ni) at 593 K under various hydrogen pressures. In the beginning, the hydriding rate is extremely high. The sample has similar hydriding rates under different hydrogen pressures. The value of H_a under 12 bar H_2 after 60 min was 4.05 wt.% hydrogen.

Fig. 5 shows the H_a versus t curves for the activated Mg-10 wt.% (Fe_2O_3, Ni) under 12 bar H_2 at different temperatures. As the temperature goes up, the hydriding rate becomes higher. However, from 40 to 60 min the hydriding rate at 593 K is higher than that at 603 K. The curve of 603 K was obtained later than that of 593 K. The maintenance of relatively high temperatures between 573 and 603 K during hydriding and dehydriding cycling and the weight of particles themselves are considered to bring about the sintering of particles, leading to the agglomeration of particles. Later measurement gives lower hydriding rate than the earlier measurement because of the decrease in the surface area of the sample.

Fig. 6 shows the variations of weight percentage of hydrogen H_d desorbed by the activated Mg-10 wt.% (Fe_2O_3, Ni) as a function of time t at 593 K with hydrogen pressures. The percentage of desorbed hydrogen H_d is expressed with respect to the sample weight. Before obtaining these curves, the sample was hydrided for 1 h under 12 bar H_2 at 593 K. As the hydrogen pressure becomes lower, the dehydriding rate goes up. Under 1.0 bar H_2, the value of H_d after 60 min was 3.05 wt.% hydrogen at 593 K.

Fig. 7 shows the variations of weight percentage of hydrogen H_d desorbed by the activated Mg-10 wt.% (Fe_2O_3, Ni) as a function of time t at 593 and 603 K under 1.0 bar H_2. The H_d value after 60 min was 3.69 wt.% at 603 K.

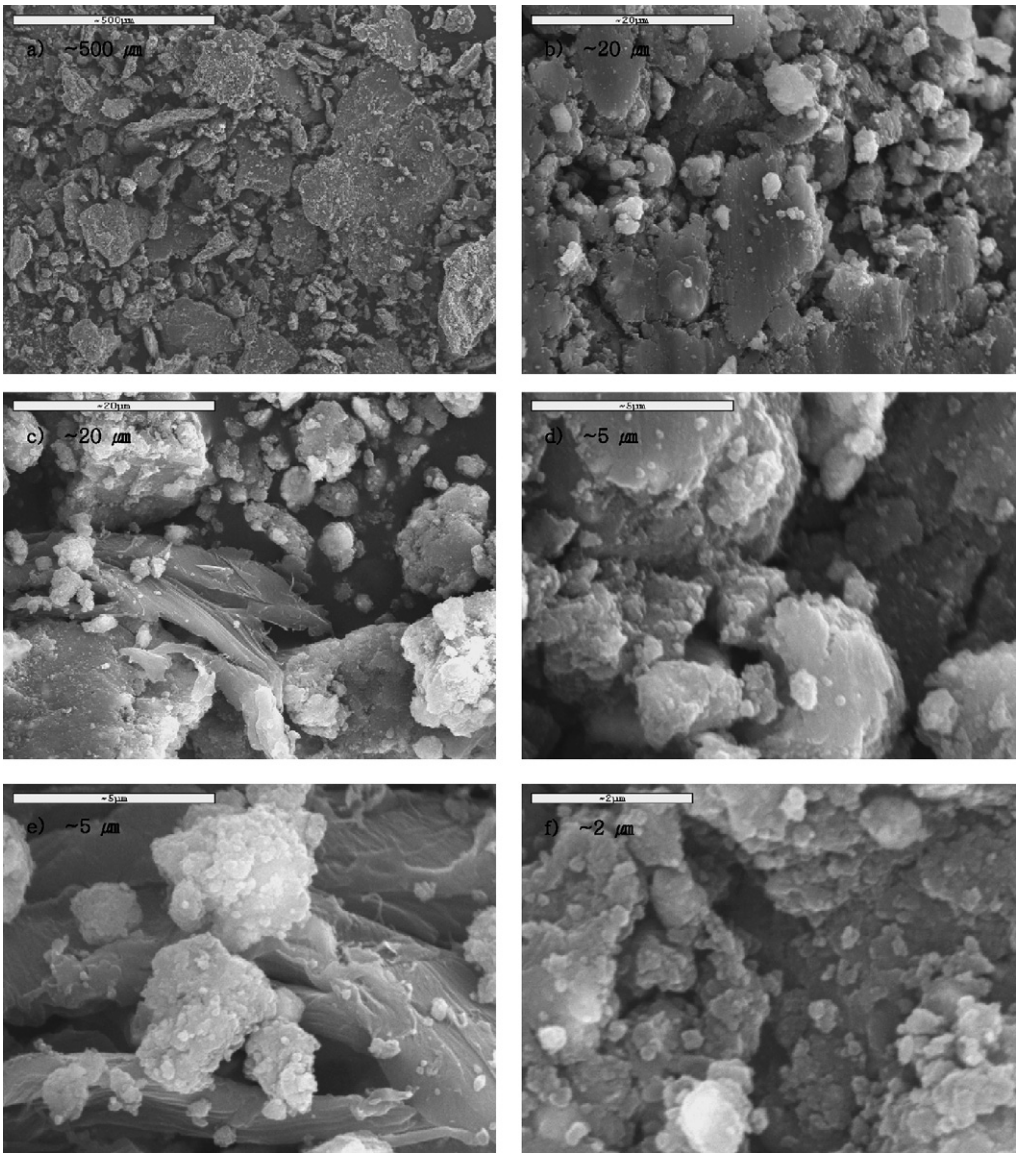

Fig. 2. Microstructures observed by SEM of Mg-10 wt.% (Fe_2O_3, Ni) as milled at different magnifications.

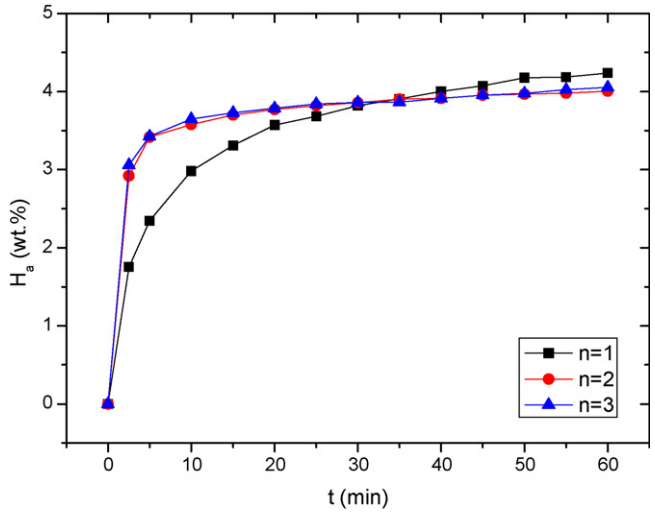

Fig. 3. Variation of H_a vs. t curve for Mg-10 wt.% (Fe_2O_3, Ni) at 593 K under 12 bar H_2 with number of cycles.

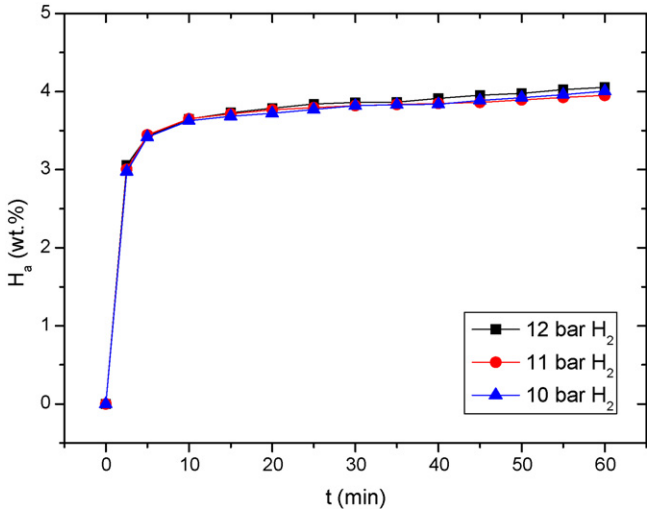

Fig. 4. Variation of H_a vs. t curve for activated Mg-10 wt.% (Fe_2O_3, Ni) at 593 K with hydrogen pressure.

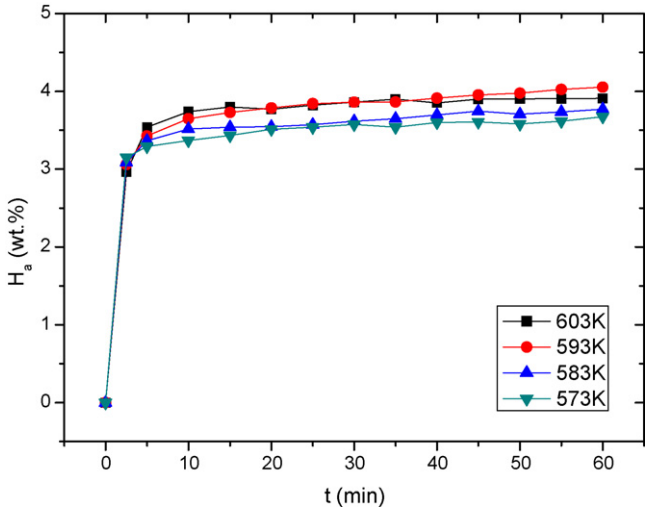

Fig. 5. Variation of H_a vs. t curve for activated Mg-10 wt.% (Fe_2O_3, Ni) under 12 bar H_2 with temperature.

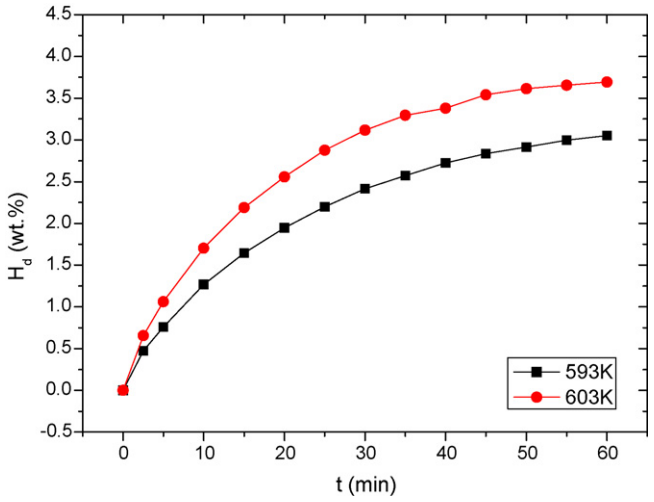

Fig. 7. H_d vs. t curves at 593 and 603 K under 1.0 bar H_2 after activation for Mg-10 wt.% (Fe_2O_3, Ni).

Fig. 8 gives the desorption pressure–composition isotherm (P–C–T curve) of the activated Mg-10 wt.% (Fe_2O_3, Ni) at 593 K. Before obtaining the data for the curve, the sample was hydrided for approximately 24 h at 593 K. The data points were obtained every 2 h. Hydrogen-storage capacity under 12 bar H_2 at 593 K is 4.85 wt.% for Mg-10 wt.% (Fe_2O_3, Ni). The plateau exhibits a slight slope. The Equilibrium plateau pressure is not clear, but it is deemed to be about 1.7 bar H_2. This Equilibrium plateau pressure is considered to correspond to that for the Mg-H_2 system. The sample has two hydride phases MgH_2 and Mg_2NiH_4 which have different equilibrium plateau pressures. Mg_2NiH_4 has higher equilibrium plateau pressures (4.99 bar H_2 at 593 K [17]) than MgH_2. However, a plateau at about 5.0 bar H_2 is not observed. Too small fraction of Mg_2NiH_4 is considered to lead to this result.

Fig. 9 gives the X-ray (Cu Kα) powder diffraction pattern of the dehydrided Mg-10 wt.% (Fe_2O_3, Ni) after 22 hydriding–dehydriding cycles. It contains Mg, Fe, Mg_2Ni and MgO. This shows that Fe_2O_3 was reduced, Mg_2Ni was formed by the reaction of Mg with Ni during hydriding–dehydriding cycling, and a small part of Mg was oxidized.

Fig. 10 shows the microstructure observed by SEM of the Mg-10 wt.% (Fe_2O_3, Ni) after 22 hydriding–dehydriding cycles, in different magnifications. The sample consists of very small particles, agglomerates of the very small particles, and large particles with smooth surfaces. The large particles with smooth surfaces are deemed to be composed of Mg. The sample after hydriding–dehydriding cycling has smaller particles than the as-milled sample.

The oxide Fe_2O_3 is brittle, and thus it is considered to be pulverized during reactive mechanical grinding. The added Fe_2O_3 and/or their pulverization during reactive mechanical grinding are considered to help the particles of magnesium become finer. The added Ni is also considered to make the particles finer by being mixed with Mg. Hydrides are also brittle. The Mg hydride formed during reactive mechanical grinding is thus considered to be pulverized during reactive mechanical grinding.

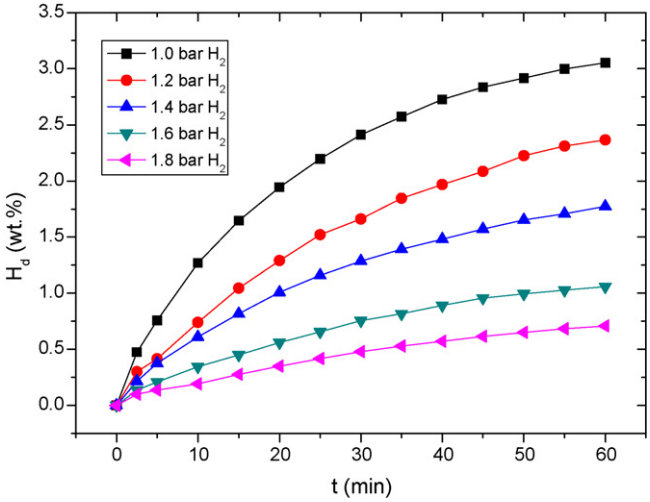

Fig. 6. Variation of H_d vs. t curve for activated Mg-10 wt.% (Fe_2O_3, Ni) at 593 K with hydrogen pressure.

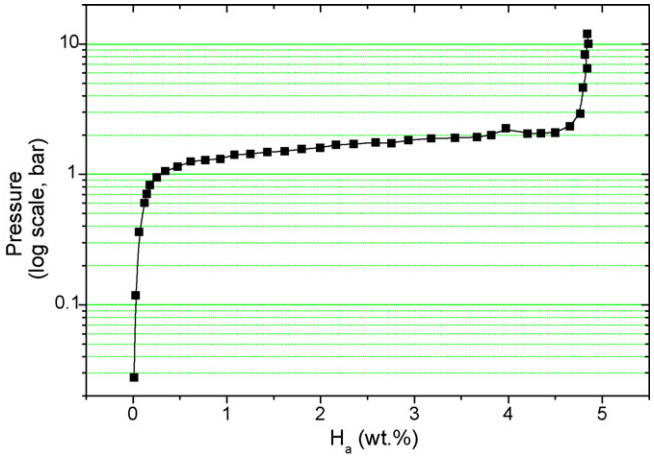

Fig. 8. Desorption P–C–T curve of the activated Mg-10 wt.% (Fe_2O_3, Ni) at 593 K.

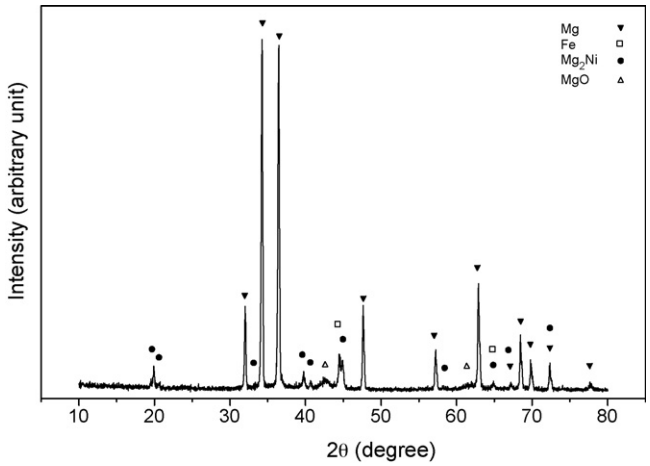

Fig. 9. X-ray (Cu Kα) powder diffraction pattern of dehydrided Mg-10 wt.% (Fe_2O_3, Ni) after 22 hydriding–dehydriding cycles.

The added Ni reacts with Mg to form the Mg_2Ni phase during hydriding and dehydriding cycling. Mg_2Ni has higher dehydriding and dehydriding rates than Mg.

The hydrogen-storage materials expand during the hydriding reaction and contract during the dehydriding reaction. This will make their particles finer and create defects on the surface and in the interior of the materials.

The reactive grinding of Mg with Fe_2O_3 and Ni and hydriding–dehydriding cycling are considered to increase the hydriding and dehydriding rates by facilitating nucleation (by creating defects on the surface of the Mg particles and by the additive) and by reducing the particle size of Mg and thus by shortening the diffusion distances of hydrogen atoms. The Mg_2Ni phase formed by the reaction of Mg with Ni is also considered to contribute to the increase of the hydriding and dehydriding rates of the sample Mg-10 wt.% (Fe_2O_3, Ni).

At 593 K under 12 bar H_2 for 60 min, the Mg-10 wt.% (Fe_2O_3, Ni) absorbed 4.05 wt.% H_2, while the Mg-10 wt.%

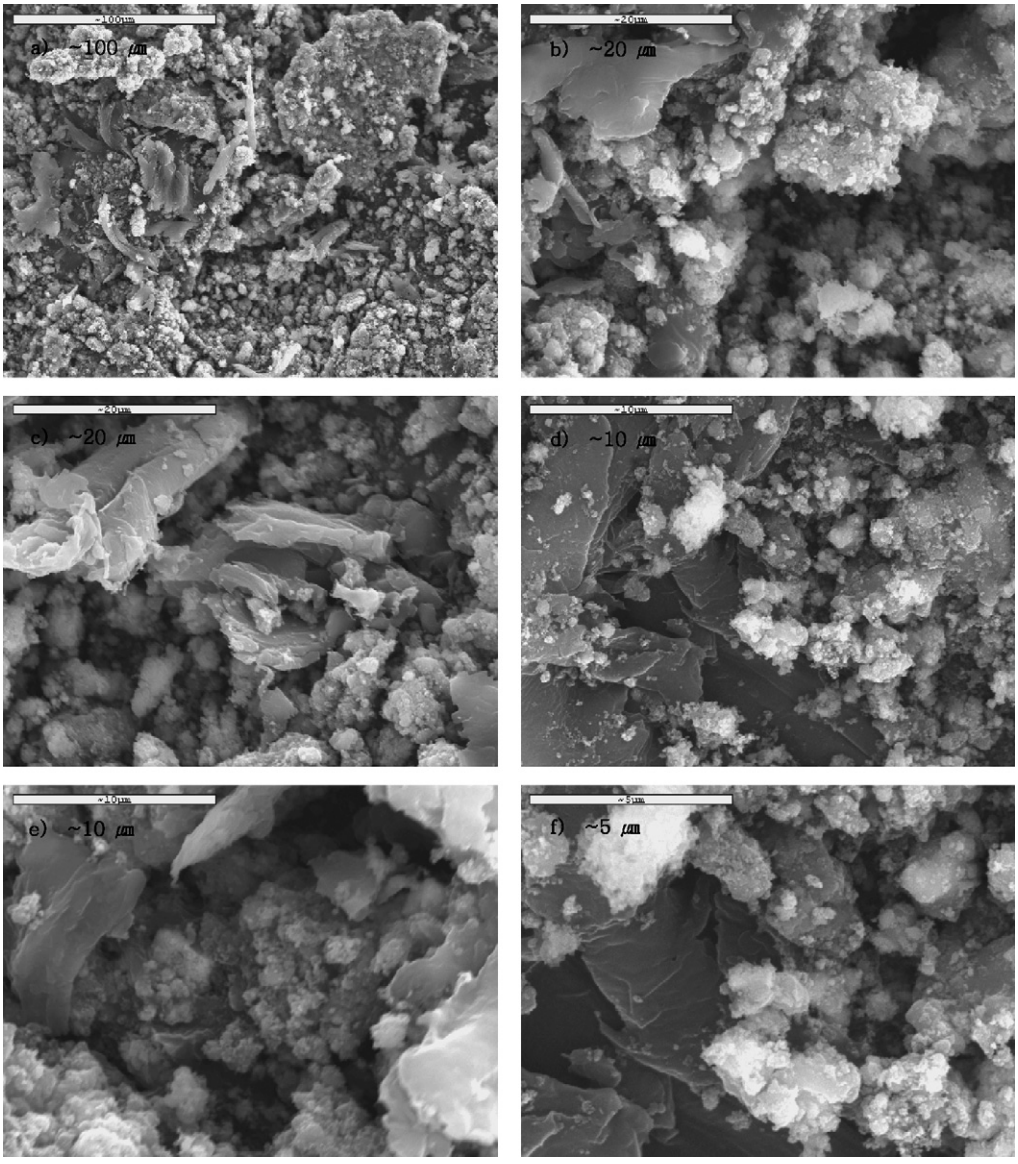

Fig. 10. Microstructures observed by SEM of Mg-10 wt.% (Fe_2O_3, Ni) after 22 hydriding–dehydriding cycles.

Fe_2O_3 by spray conversion absorbed 5.55 wt.% H_2. At 593 K 1.0 bar H_2 for 60 min, the Mg-10 wt.% (Fe_2O_3, Ni) desorbed 3.05 wt.% H_2, whereas the Mg-10 wt.% Fe_2O_3 by spray conversion desorbed 1.04 wt.% H_2. Mg-10 wt.% (Fe_2O_3, Ni) has a smaller hydriding rate than Mg-10 wt.% Fe_2O_3 by spray conversion, but it has a much higher dehydriding rate than the Mg-10 wt.% Fe_2O_3 by spray conversion. This is considered to be due to the Mg_2Ni phase formed by the reaction of Mg with Ni during hydriding–dehydriding cycling, which has a higher dehydriding rate than Mg. The Mg_2Ni phase plays a catalytic role for the decomposition of MgH_2. The faster decomposition of Mg_2Ni hydride than Mg hydride is considered to increase the dehydriding rate of MgH_2 by facilitating the nucleation of α-solid solution of hydrogen in Mg and initiating the decomposition of MgH_2. In addition, the contraction of Mg_2Ni by decomposition from its hydride is considered to provide the passage of hydrogen decomposed from the Mg hydride, leading to the increase in the dehydriding rate of Mg hydride.

4. Conclusions

The sample Mg-10 wt.% (Fe_2O_3, Ni) was prepared by grinding Mg mechanically under H_2 (reactive mechanical grinding) with ultrafine Fe_2O_3 particles and Ni particles. The sample Mg-10 wt.% (Fe_2O_3, Ni) as milled absorbed 4.24 wt.% hydrogen at 593 K under 12 bar H_2 for 60 min. Its activation was accomplished only by one hydriding–dehydriding cycle. The activated sample absorbed 4.05 wt.% hydrogen at 593 K, 12 bar H_2 for 60 min and desorbed 3.05 wt.% hydrogen at 593 K, 1.0 bar H_2 for 60min. After hydriding–dehydriding cycling, Fe_2O_3 was reduced, Mg_2Ni was formed by the reaction of Mg with Ni, and a small fraction of Mg was oxidized. The reactive grinding and the Mg_2Ni phase formed by the reaction of Mg with Ni are considered to contribute to the increase of the hydriding and dehydriding rates of the sample Mg-10 wt.% (Fe_2O_3, Ni).

Acknowledgements

This research was performed for the Hydrogen Energy R&D Center, one of the 21st Century Frontier R&D Program, funded by the Ministry of Science and Technology.

References

[1] M.Y. Song, J. Mater. Sci. 30 (1995) 1343.
[2] M.Y. Song, E.I. Ivanov, B. Darriet, M. Pezat, P. Hagenmuller, Int. J. Hydrogen Energy 10 (3) (1985) 169.
[3] M.Y. Song, E.I. Ivanov, B. Darriet, M. Pezat, P. Hagenmuller, J. Less-Common Met. 131 (1987) 71.
[4] M.Y. Song, Int. J. Hydrogen Energy 20 (3) (1995) 221.
[5] J.-L. Bobet, E. Akiba, Y. Nakamura, B. Darriet, Int. J. Hydrogen Energy 25 (2000) 987.
[6] A.R. Yavari, A. Lemoulec, F.R. De Castro, S. Deledda, O. Friedrichs, W.J. Botta, G. Vaughan, T. Klassen, A. Femandez, A. Kvick, Scripta Mater. 52 (8) (2005) 719.
[7] J. Huot, M.-L. Tremblay, R. Schulz, J. Alloy Compd. 356–357 (2003) 603.
[8] H. Imamura, M. Kusuhara, S. Minami, M. Matsumoto, K. Masanari, Y. Sakata, K. Itoh, T. Fukunaga, Acta Mater. 51 (20) (2003) 6407.
[9] M.Y. Song, I.H. Kwon, S.N. Kwon, C.G. Park, H.R. Park, J.S. Bae, Int. J. Hydrogen Energy 31 (2006) 43.
[10] M.Y. Song, I.H. Kwon, S.N. Kwon, C.G. Park, S.H. Hong, D.R. Mumm, J.S. Bae, J. Alloy Compd. 415 (1–2) (2006) 266.
[11] M.Y. Song, Int. J. Hydrogen Energy 20 (3) (1995) 221.
[12] M.Y. Song, J. Mater. Sci. 30 (1995) 1343.
[13] M.Y. Song, J.-P. Manaud, B. Darriet, J. Alloy Compd. 282 (1998) 243.
[14] M.Y. Song, Int. J. Hydrogen Energy 28 (2003) 403.
[15] M.Y. Song, D.S. Lee, I.H. Kwon, Met. Mater. Int. 10 (1) (2004) 69.
[16] M.Y. Song, D.S. Ahn, I.H. Kwon, H.J. Ahn, Met. Mater. Int. 5 (5) (1999) 485.
[17] M.Y. Song, H.R. Park, J. Alloy Compd. 270 (1998) 164.